Measurements of Interfacial Strength from the Blister Test

CHI WANG

Department of Chemical Engineering, Yuan-Ze University, Neili, Taoyuan, Taiwan 320, R.O.C.

Received 2 September 1998; accepted 29 December 1998

ABSTRACT: Measurements of the interfacial properties between an elastic tape and poly(methyl methylcrylate) substrates were carried out using a circular blister test. All properties, including adhesive fracture energy G_a, residual stress σ_o and the elastic modulus of the tapes can be deduced in a single test. Three different approaches have been adopted to analyze the relations between blister radius, blister height, and the pressure inside the blister. A comparison of the calculated results from these methods is provided and the details of the fracture process are discussed. Effect of the volume flowrate of the injected fluid was investigated as well. Results show that the deduced value of G_a is about 3.0 ± 0.5 J/m^2 and the elastic modulus of tape is 330 ± 40 MPa, in good agreement with that determined from the tensile test. The fracture time is reduced from 4000 to 700 s for a flowrate of the injected fluid from 0.05 to 0.5 mL/h. In all cases, quasistatic deformation of the blister is found valid and the effect of the flowrates on the failure mechanics is not significant for the present study. However, one should take the dynamic deformation effect of the blister into consideration when the flowrate is too high. © 1999 John Wiley & Sons, Inc. J Appl Polym Sci 73: 1899–1912, 1999

Key words: blister test; adhesive fracture energy; thin films; residual stress

INTRODUCTION

Bonding of polymeric thin films onto rigid substrates is an important issue in determining the performance of the composite systems. Especially in the IC industry, the adhesion between the photoresist and the silicon substrate is a crucial problem in consideration of the duration and high temperature environments. There are many testing methods[1–7] to quantitatively characterize the interfacial strength, either by fracture stress criterion or by fracture energy criterion. Among all, the peel test is the most popular one both in the industry and in the academy. It is attributed to the simple sample preparation and data analysis. The measured interfacial strength is termed adhesive fracture energy G_a, which is defined as the energy required to separate unit area at the interface. When carrying out the peel test, however, the peel adherent requires certain mechanical strength to avoid the failure of the adherent itself. Otherwise, the failure locus is not at the interface, but in the film itself, which makes the measurement of the interfacial strength unfeasible. Polymeric thin films (thickness smaller than 50 μm) are usually delicate and deform easily under tension. Moreover, it has been pointed out that bending effect on the measured peel force is pronounced when rigid adherents are peeled.[8] The dissipative energy caused by viscoelastic effect of the bended adherent sometimes is significant compared with the true adhesive fracture energy. Under certain circumstances, the peel test is not quite suitable to measure the interfacial strength of thin films bonded onto rigid substrates. On the other hand, the blister test provides an appropriate G_a measurement to minimize the possible dissipation energy. In the blister test, a circular

Correspondence to: C. Wang.

Contract grant sponsor: National Science Council, Republic of China.

Journal of Applied Polymer Science, Vol. 73, 1899–1912 (1999)
 CCC 0021-8995/99/101899-14

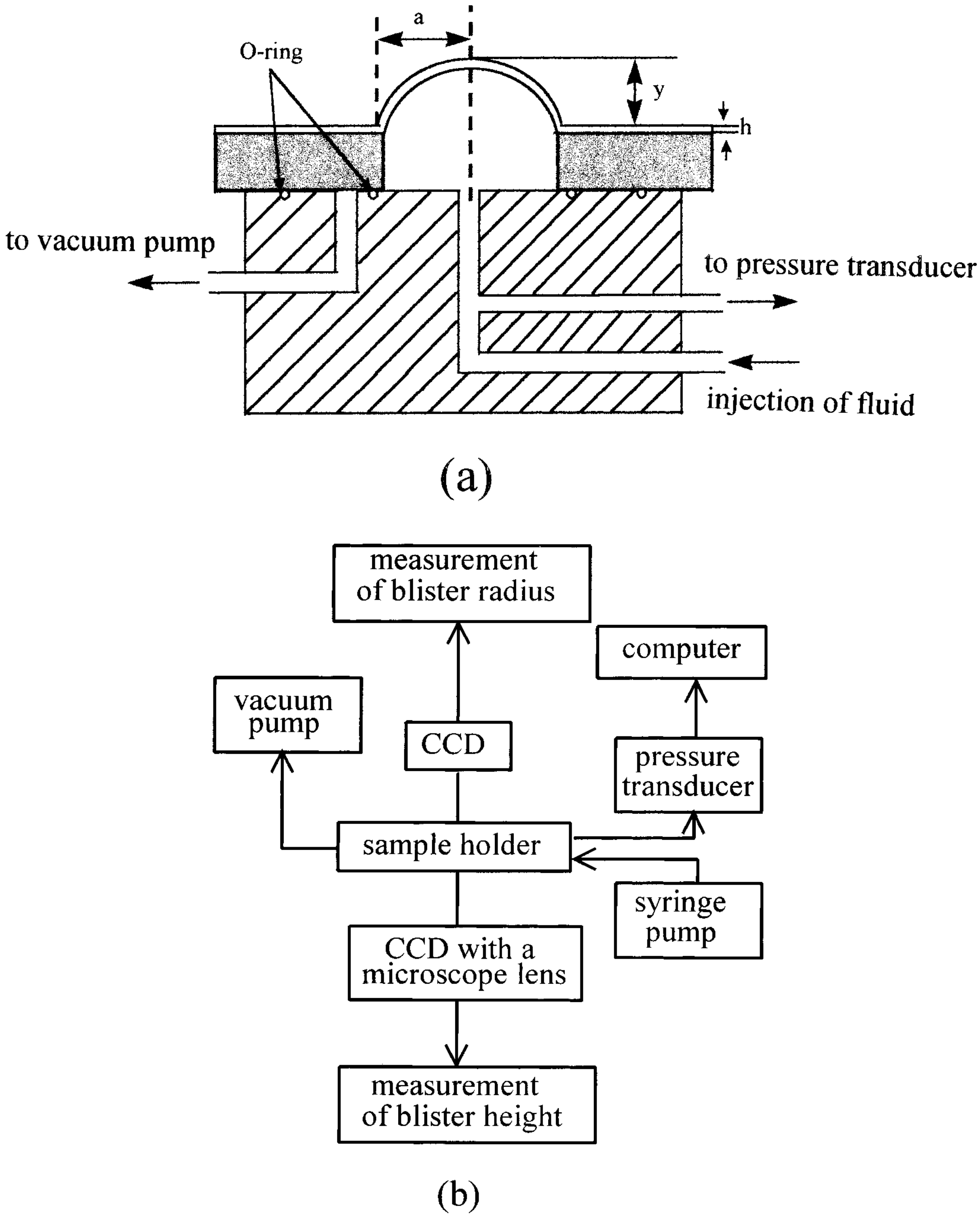

Figure 1 Schematic presentation of the blister test: (a) side view of the sample and sample holder, (b) layout of the measurements.

hole filled with fluid is overlaid by a thin film at one side and continuous injection of the fluid at the other side is conducted to blow (pressurize) the film. Thus, the film is pressurized to form a "blister". A circular debond starts to grow when the pressure inside the blister reaches a critical value. By measuring the height of the blister, radius of the circular debond and the pressure inside the blister, the values of adhesive fracture energy and the residual stress of the thin film can be deduced. The first report on the blister test for adhesion measurement was credited to Dannenberg[9] in 1961. Blister test has been widely applied to determine the interfacial strength of film/substrate pairs, such as polyurethane/Al,[10] elastic tapes/glass,[11] polystyrene/silica,[12] photopolymer/

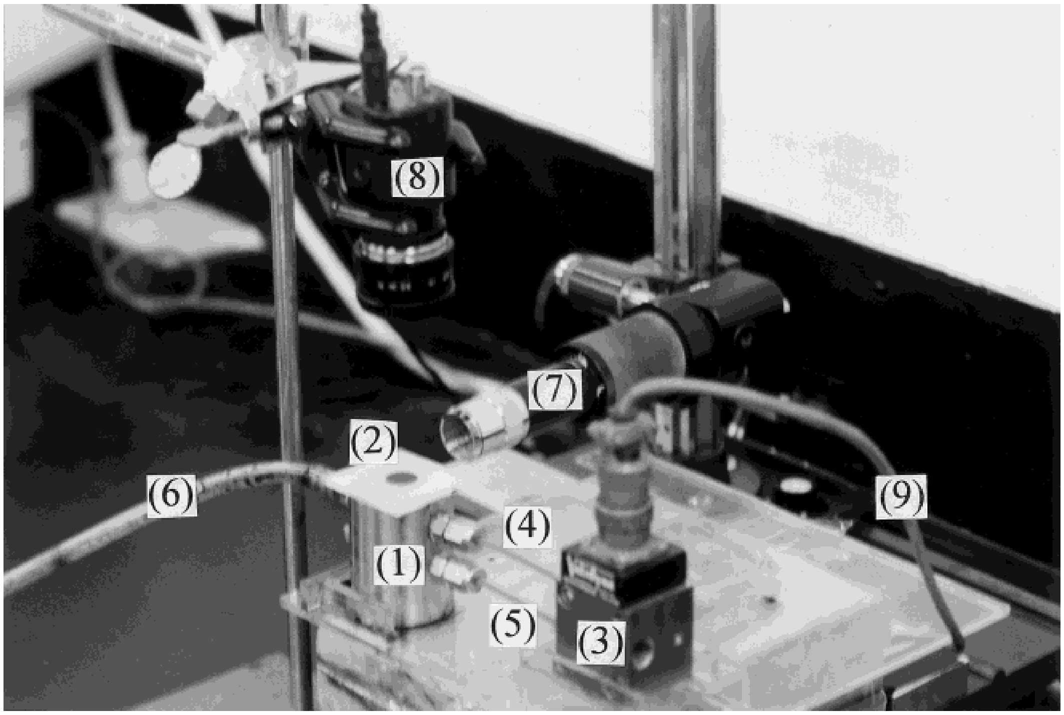

Figure 2 A photograph of the apparatus for blister test: (1) sample holder, (2) sample, (3) pressure transducer, (4) line to the pressure transducer, (5) line to the syringe pump, (6) vacuum line, (7) CCD with a microscope lens for blister height measurements, (8) CCD for blister radius measurements, and (9) line to a personal computer.

glass fiber-reinforced plastics,[13] polyimide/silica,[14] and *cis*-polyisoprene/polymethylmethacrylate.[15] Recently, Allen et al.[16] have discussed the limitation of blister test and presented another feature (island blister) for adhesion measurements.

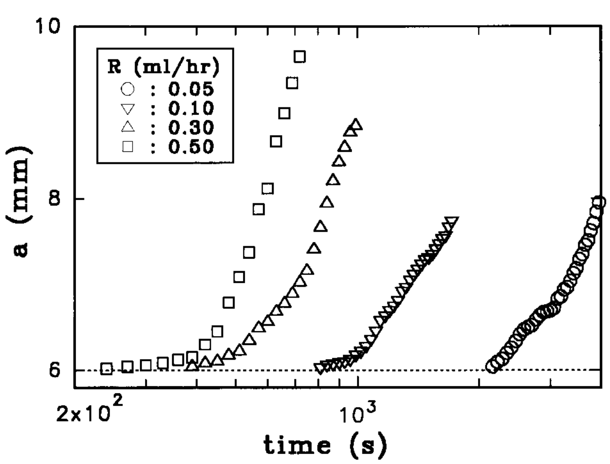

Figure 3 Variation of the blister radius a during the test.

For the ceramic coating layer (thin hard films), however, the microscratch test[17] has become the common method to determine the adhesive strength. In this test, scratches are produced on the sample using a diamond stylus. The adhesive strength is characterized as the critical load, which causes the damage to take place when the stylus drawn across the sample under increasing load. In contrast to the blister test, it is difficult to express the level of adhesion quantitatively by using microscratch test because the critical load depends not only on the strength of the interface, but also on the test geometry and mechanical properties of the coating layer. On the other hand, the adhesive fracture energy determined using the blister test is independent of the test geometry.[1,11] It has been pointed out the adhesive fracture energy of the polymeric systems is correlated with the testing rate and the temperature in accordance with the principle of rate-temperature superposition.[2,4] However, the effect of the debonding rate (flowrate of the injected fluid) on the adhesive fracture energy measured by the blister test has not yet been investigated to the author's knowledge. Thus, the objective of this

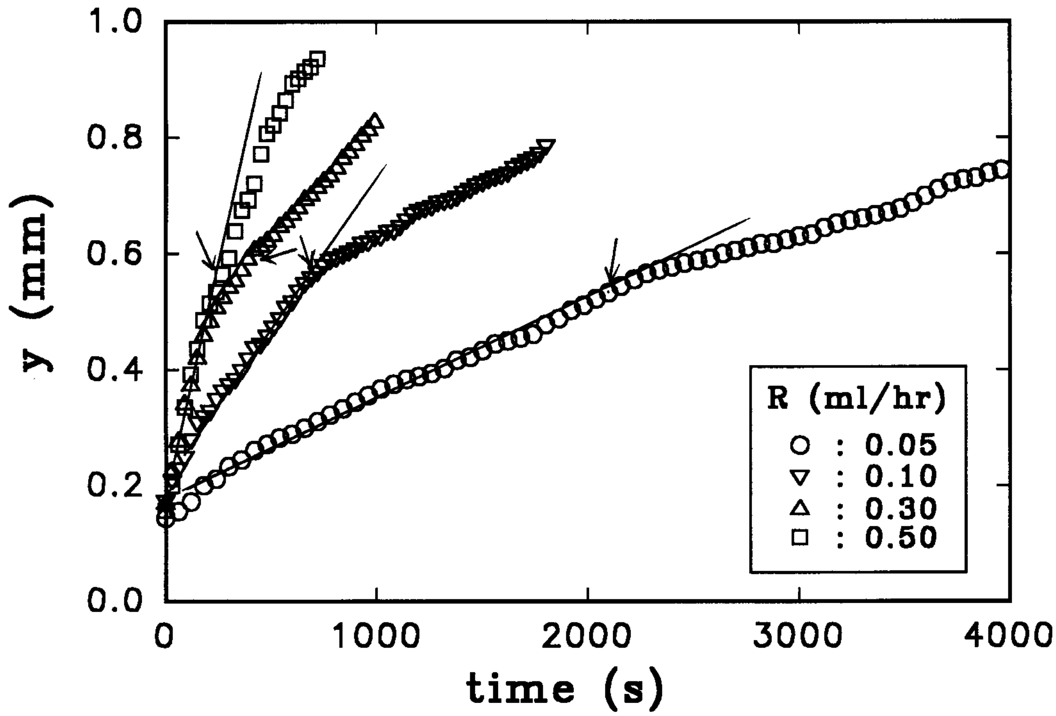

Figure 4 Variation of the blister height y during the test (the arrows pointing to the critical height y_c, where initial debonding takes place).

work is to elucidate the effect of the debonding rate on the fracture behavior of a pressurized blister.

Theoretical Consideration

Before Debonding

The schematic presentation of the blister test is shown in Figure 1a. We consider a thin elastic film (membrane) bonded onto a rigid substrate. A linear relation between the volume of blister V and the height of the blister y is expressed, according to the theory of classical elasticity, as follows[9]

$$V = C_1 \pi a_o^2 y \tag{1}$$

where a_o is the radius of the initial blister and C_1 is a constant equal to 0.519. Moreover, the pressure P inside the blister is derived to be[13,16]

$$P = \frac{3.56Ehy^3}{a_o^4} + \frac{4h\sigma_o y}{a_o^2} \tag{2}$$

where E is the elastic modulus of the thin film, h is the thickness of the film, and σ_o is the residual stress at the interface. The origin of the residual stresses is attributed to the thermal stresses induced by a mismatch of the thermal expansion coefficients between the film and the substrate after they are bonded each other. Thus, a plot of P/y versus y^2 will give a straight line whose slope and intercept are determined and used to calculate the elastic modulus E and residual stress σ_o respectively.

After Debonding

After debonding, growth of the blister radius is observed. The interfacial strength can be characterized by the amount of energy G_a required to propagate a crack by unit area. Three methods have been provided to analyses the fracture behavior and determine the values of G_a: (1) Fernando and Kinloch,[13] (2) Gent and Lewandowski,[11] and (3) Chu and Durning[15] methods. Each one has its own advantages.

Fernando and Kinloch (FK) method.[13] When the initial circular crack a_o starts to grow at a critical

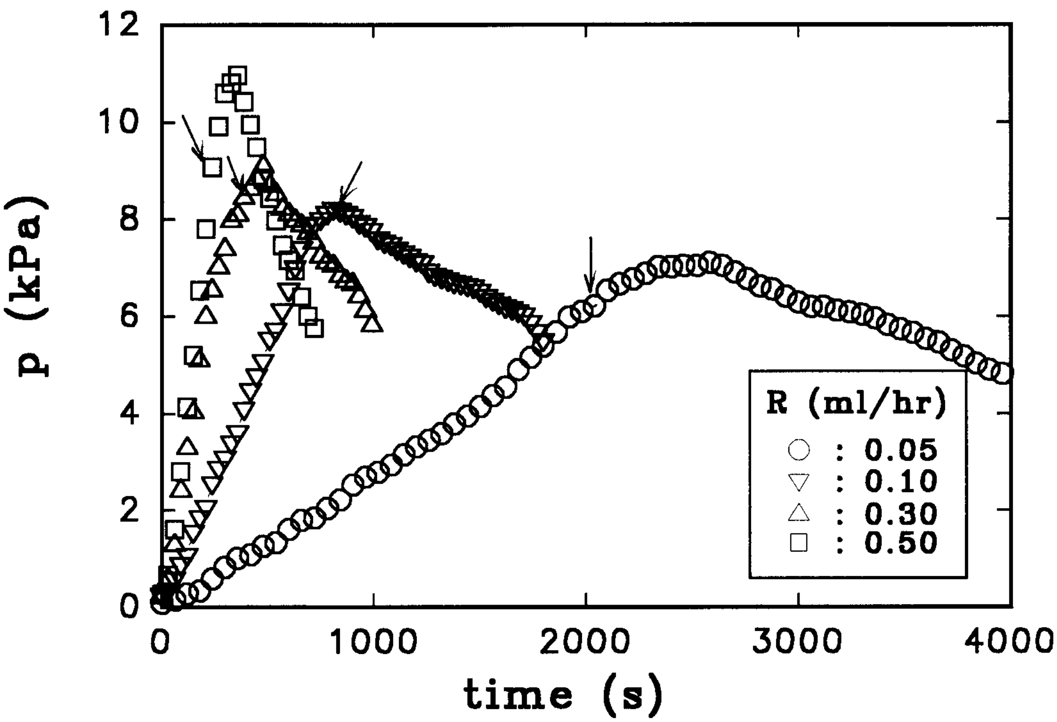

Figure 5 Variation of pressure inside the blister P during the test (the arrows pointing to the critical pressure, p_c, where initial debonding takes place).

time t_c, the adhesive fracture energy G_a has been derived as follows,[13,16]

$$G_a = \frac{2.22Ehy_c^4}{a_o^4} + \frac{2h\sigma_o y_c^2}{a_o^2} \quad (3)$$

where y_c is the height of the blister when debonding takes place. Thus, value of G_a is deduced by simply measuring the critical height y_c and then substituting into eq. 3. The contribution of residual stresses to the adhesion can be neglected when the ratio of the second term to the first term in eq. 3 is very small, i.e., $1.12\,(\sigma_o/E)\,(a_o/y)^2 \ll 1$.

Table I Measured Values of C_1 and Slopes of the Plots Log P Versus Log y for Different Flowrates R

R (mL/h)	dy/dt (μm/s)	Value of C_1	Slope
0.05	0.213	0.57	3.02
0.1	0.507	0.49	2.97
0.3	1.43	0.52	2.85
0.5	1.78	0.69	2.78

Gent and Lewandowski (GL) method.[11] Using Griffith's fracture criterion, debonding takes place when the net available energy, i.e., the work done by the injection of fluid minus the energy stored in the elastic thin film, is larger than the work for the interfacial detachment. Gent et al.[11] has derived eqs. 4 and 5 to describe the level of adhesion, based on an energy balance

$$G_a = 0.649Py \quad (4)$$

$$Pa = (1.74EhG_a^3)^{1/4} \quad (5)$$

where a is the radius of the debonded circular crack. One should know that eqs. 4 and 5 are derived without considering the effect of residual stress. As pointed out previously,[13,16] a similar equation, $G_a = 0.624Py$, can be derived from eq. 3 if the residual stress is neglected.

According eqs. 4 and 5, the product of the pressure inside the blister and the height of the blister (or the blister radius) is constant after debonding takes place. Thus, the adhesive fracture energy can be determined simply using eq. 4. Moreover, the elastic modulus of the elastic film can be determined using eq. 5 after deriving G_a from eq. 4.

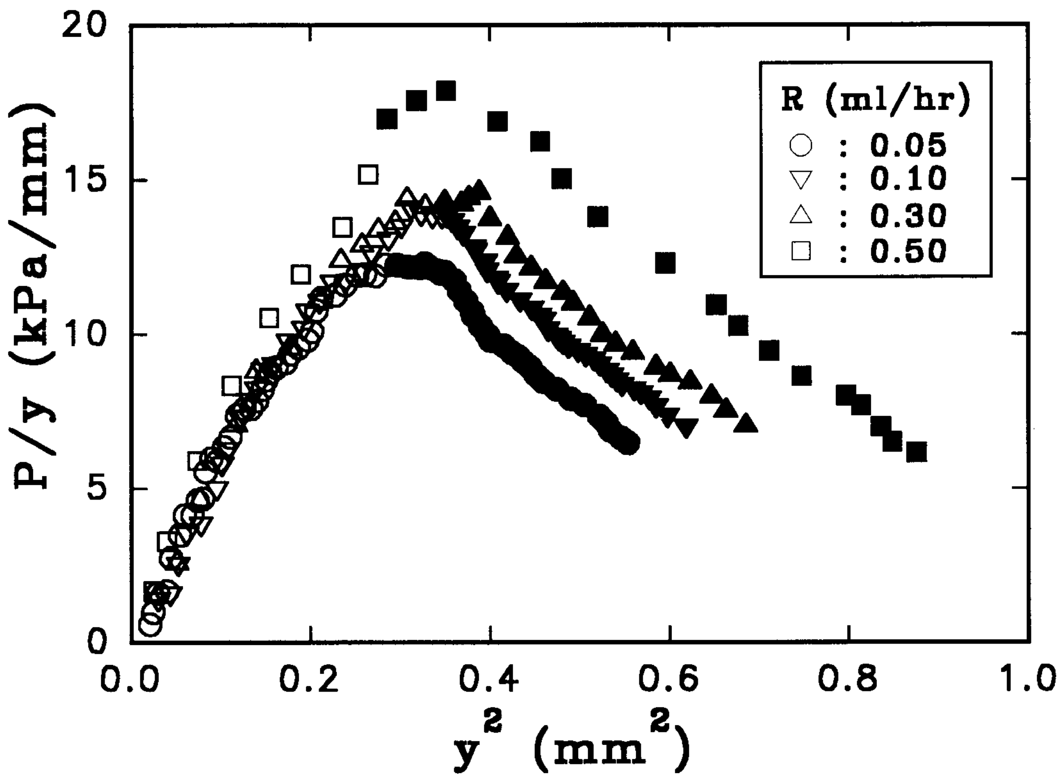

Figure 6 Plot of P/y versus y^2, according to eq. 2 (open symbols: before debonding; filled symbols: after debonding).

Chu and Durning (CD) method.[15] When the fluid is injected into a growing blister continuously with a volume flowrate of R, eqs. 6, 7 and 8 are derived, based on the Gent's theory, to determine the value of G_a,

$$G_a = 0.44Eh(R/M)^4 \tag{6}$$

$$G_a = 8.18Eh(L/R)^2 \tag{7}$$

$$G_a = 0.39(R^2/N^2Eh)^{0.2} \tag{8}$$

where M, L, and N are the slopes of the plots of a^3 versus $t - t_c$, y^3 versus $t - t_c$ and P^{-3} versus $t - t_c$, respectively. The t_c is the critical time for a debond to initiate. Again, the residual stress is not taken into account in deriving eqs. 6–8.

EXPERIMENTAL

Sample Preparation

Polymeric tapes, about 50 μm thick, were used as the elastic thin films. PMMA plates, 40 × 32 × 3 mm^3, were used as the rigid substrates. A circular hole with a diameter of 12 mm was made at the center of the PMMA plate. Then, the elastic tape was bonded gently to the PMMA plate with a great care to avoid any air trapped at the interface. Great attention has been also given to the vicinity of the substrate perforation to ensure the reproducible results. Forming a vacuum between the two O-rings, as shown in Figure 1a, a sample holder similar with that developed by Chu et al.[15] was used to hold the sample firm during the test.

Measurements

The selection of the injected fluid is rather important in order not to induce any variation of the interface. Distilled water dyed with black pigment was found suitable and was injected into the blister using a syringe pump at different flowrates R (0.05 ~ 0.5 mL/h). The pressure in the blister was measured with a pressure transducer (UPC607, Validyne), which was connected to a PC computer for the data storage. During the test, the height y and the radius a of the blister were monitored and recorded with two CCDs, as shown

Table II Measured Values Using the FK Method

R (mL/h)	E (MPa)	σ_o (MPa)	y_c (mm)	P_c (kPa)	G_a (J/m^2)
0.05	321	0.22	0.54	6.5 ± 0.1	2.52
0.1	296	0.28	0.59	8.16 ± 0.12	3.34
0.3	315	0.25	0.59	8.34 ± 0.06	3.39
0.5	394	0.25	0.53	8.45 ± 0.02	2.66

in Figure 1b. Because the variation of the blister height is rather small, a microscope lens was fitted to the CCD for the height measurement. Thus, the accuracy for the height and radius measurement is about 6 and 100 μm, respectively. Before measurements, the pressure is calibrated with an open-end U tube manometer and the length scale is calibrated with a stage micrometer. Figure 2 is the photograph of the testing apparatus. After a test, the height and radius of the deformed blister during the test were measured using an image processing analyzer.

For each fluid flowrate, two measurements were carried out and good reproducibility of the results was obtained.

RESULTS AND DISCUSSION

Figure 3 shows the variation of blister radius a with time when the fluid is injected continuously at different flowrates R. The initial blister radius a_o is 6 mm shown by the dotted line. Thus, the onset of the initiation of a debond is easily determined. Initially, a slow growth of blister radius is evident, followed by a fast growth at the late stage of debonding. Similar fracture behavior has been found by Fernando et al.[13] In contrast, a decreasing growth rate of blister radius was detected by Chu et al.[15] with an injected rate of 3 mL/h. They attributed the reduction in the debonding rate to an inertial effect at the vicinity of the substrate perforation where the interface was critical. In the present study, the injection of the fluid (thus, the increase of the blister volume) is so small (0.05–0.5 mL/h) that inertial effect is assumed to be negligible. Moreover, growth of a well-defined circular crack, observed from the top view, is developed exclusively when the interface is well controlled. If the interfacial strength at the circum-

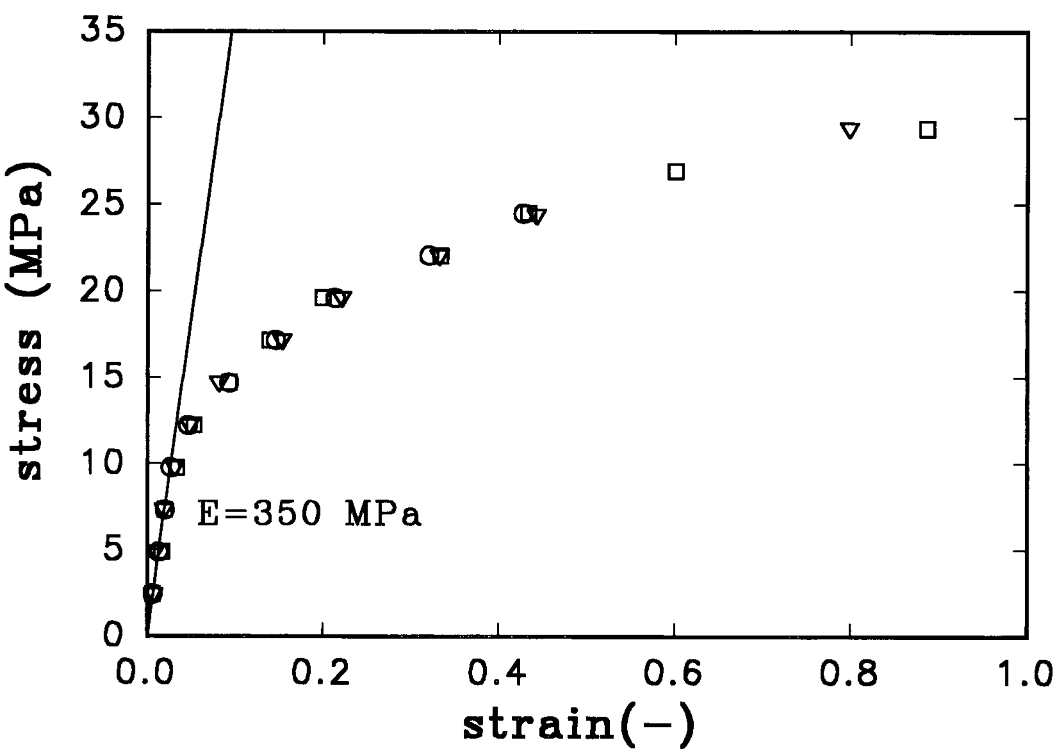

Figure 7 Stress–strain curve for the elastic tape.

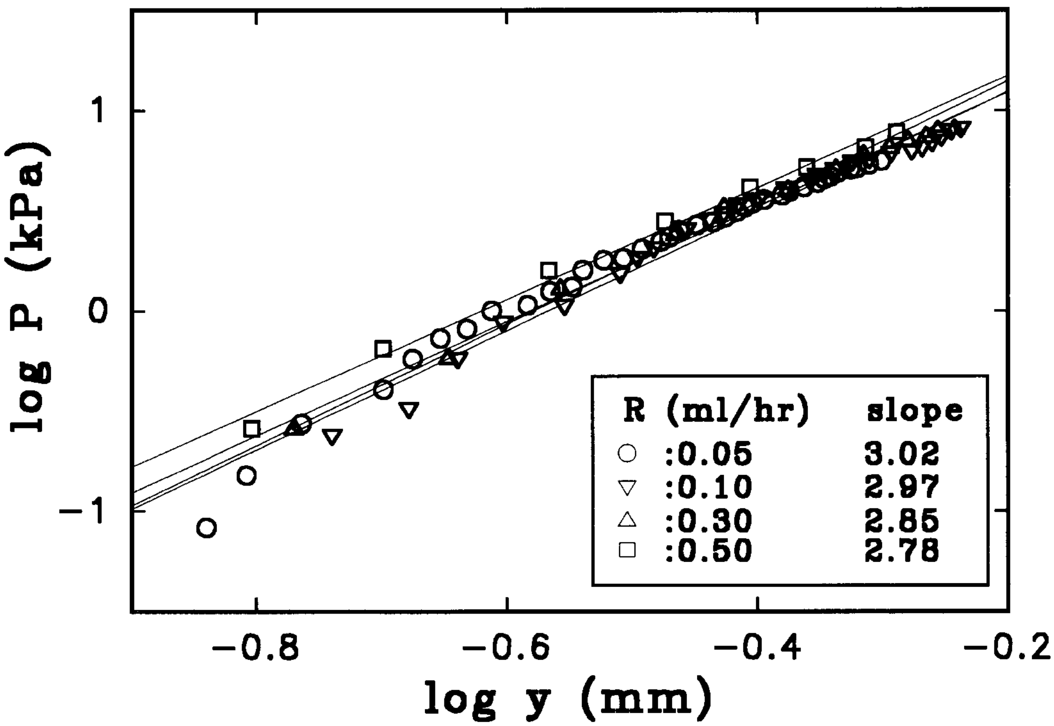

Figure 8 Variation of pressure inside the blister P versus blister height y before debonding.

ference of the blister is not at the same level, irregular growing fronts of the debond is detected which violates the assumptions used in deriving the relevant equations. As seen from Figure 3, the time to initiate a circular debond is longer for a smaller injected flowrate. The induction time is about 2130 and 225 s for 0.05 and 0.5 mL/h, respectively. It should be noted that the equations derived in the theoretical section are based on the static (equilibrium) deformation assumptions. Dynamic effects have to be taken into account when a high deformation rate is applied, especially for the polymeric materials which show viscoelastic properties. The rate of detachment of films from the substrates is by no means constant, as shown in Figure 3. Nevertheless, the detachment rate increases as the flowrate is increased.

The height at the center of the blister is measured as well during the inflation period, as shown in Figure 4. The arrows point out the onset of the initial debond. Before debonding, a linear growth of the blister height is evident, where the blister radius is 6 mm. After initiation of a debond, a change in the growth rate of the blister height is detected until a complete failure of the interface. It is interesting to know that the critical height y_c to initiate a debond is more or less constant, about 0.56 ± 0.03 mm, regardless of the flowrates used. Moreover, a small blister height at zero time was found and was attributed to the results of the compression of the rubber O-rings when the vacuum was applied to fasten the samples tightly, as shown in Figure 1a.

The variation of pressure P inside the blister is shown in Figure 5 when the fluid is injected continuously. It is apparent that the pressure increases gradually, reaches a maximum value and decreases continuously until a complete failure. Attention has been given to the critical pressure

Table III Measured Values of Apparent Debonding Rates *da/dt* and Apparent Height Growth Rate *dy/dt* After Debonding

R (mL/h)	Slow Crack Growth da/dt (μm/s)	Fast Crack Growth da/dt (μm/s)	dy/dt (μm/s)
0.05	1.05	1.32	0.11
0.1	0.57	2.12	0.19
0.3	1.91	6.20	0.39
0.5	0.88	12.17	0.72

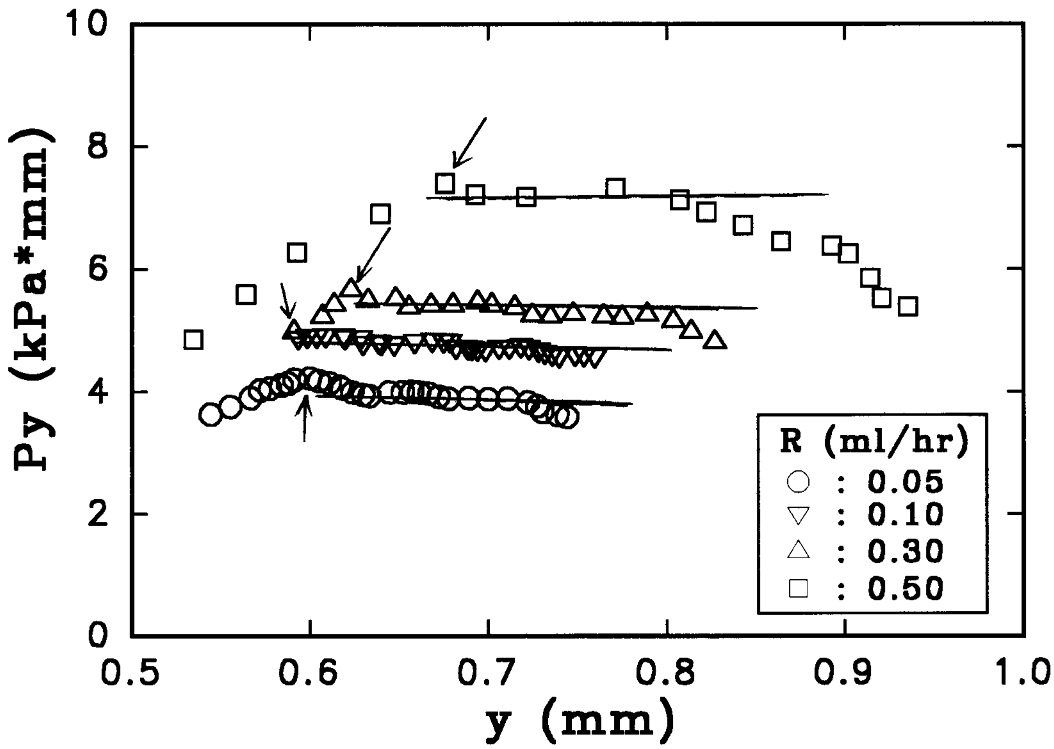

Figure 9 Plot of Py versus y after debonding, according to eq. 4 (the arrows pointing to the onset where a fast crack growth starts).

P_c where an initial debond starts. The initial debond usually takes place before a maximum pressure is reached. In addition, the value of P_c increases slightly from 6.6 to 8.4 kPa for a flowrate from 0.05 to 0.5 mL/h. On the other hand, the maximum pressures measured are 7.1 and 11.0 kPa, respectively, at the corresponding flowrates.

Before Debonding

Before debonding takes place, a linear relation between blister height and time is observed in Figure 4 where the radius of blister keeps constant a_o. By substituting the linear slope (dy/dt) into eq. 1, the constant C_1 can be determined with time derivative of volume $dV/dt = R$. The calculated values are tabulated in Table I. It seems that reasonable agreements were obtained between the experimental values and the theoretical one, 0.519. However, a relatively large value is deduced for the case $R = 0.5$ mL/h. This discrepancy could be an indication that dynamic deformation of the blister is getting more important at higher flowrates.

According to eq. 2, a plot of P/y versus y^2 will give a straight line used to deduce the interfacial properties. Figure 6 shows the effect of volume flowrate on such a plot. The open and filled symbols are results measured before and after debonding, respectively. It is evident that the maximum value of P/y increases with the flowrate. The initial slope was used to determine the elastic modulus of the polymeric tapes E and the intercept was used for measurements of the residual stress σ_o. The calculated values of E and σ_o are tabulated in Table II. It seems that elastic modulus and residual stress are independent of the flowrates, being about 330 $\pm$ 40 and 0.25 $\pm$ 0.02 MPa, respectively. It should be noted that eq. 2 is derived based on the theory of linearly elastic deformation. Thus, the strain of the tape should be less than its elastic limit to ensure the validity of eq. 2. Stress-strain relation of the tape was measured independently by stretching a dumbbell-shaped film (gauge length = 10 mm, width = 4 mm) using dead weights. As can be seen in Figure 7, the elastic strain limit of the tape is about 0.03. On comparison with the maximum strain, 2×10^{-4}, of the tape during the blister test,[12] it seems that linearly elastic deformation of the tape is certain and eq. 2 is appropriate to be

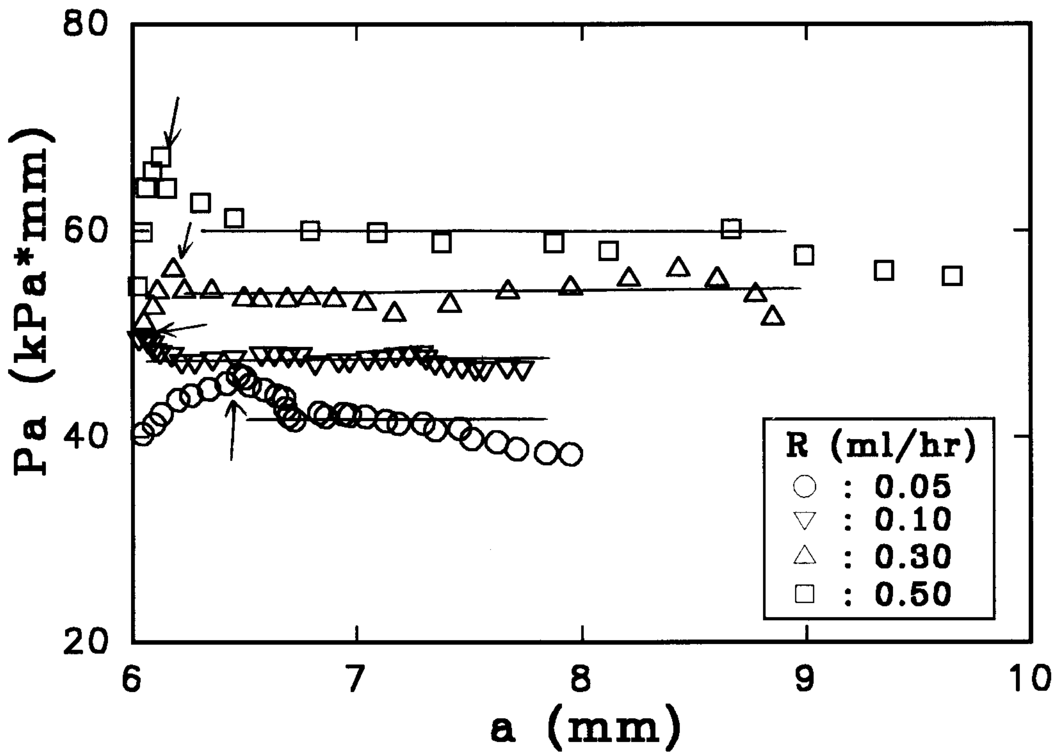

Figure 10 Plot of Pa versus a after debonding, according to eq. 5 (the arrows pointing to the onset where a fast crack growth starts).

used. Moreover, the elastic modulus determined from the small strains in Figure 7 is 350 ± 20 MPa which is in a good agreement with that obtained from the blister test, Table II.

A quite small residual stress was measured for the present system. Generally speaking, the origin of the residual stress is mainly attributed to the thermal stress created at the interface due to the temperature change and a mismatch in the thermal expansion coefficients of the bonded materials. Because there is no temperature change during the sample preparation here, insignificant residual stress at the interface is expected. Without taking the residual stress into account (i.e., the value of σ_o is set to zero in Equation 2), the log-log plot of pressure versus blister height is shown in Figure 8. Majority of the data were superposed to form a master-like curve and the linear slopes were determined and tabulated in Table I as well. It is evident the slopes are rather close to the theoretical value, 3.0, for all flowrates. A maximum relative error of 7% was found in the condition where the largest flowrate 0.5 mL/h was used. It should be noted that eqs. 1 and 2 are based on the assumption of deformation under static conditions. Quasi-static conditions seem valid for the present flowrates. However, when the flowrate is too high, the status of quasi-static deformation can not be maintained and the dynamic deformation effect of the blister has to be

Table IV Measured Values Using the GL Method

R (mL/h)	Py (kPa · mm)	Pa (kPa · mm)	G_a (J/m^2) Eq. 4	E (MPa) Eq. 5
0.05	3.94 ± 0.17	42.18 ± 2.07	2.6 ± 0.2	207 ± 71
0.1	4.73 ± 0.09	47.49 ± 0.53	3.1 ± 0.1	196 ± 21
0.3	5.32 ± 0.19	53.92 ± 1.25	3.5 ± 0.2	227 ± 44
0.5	6.60 ± 0.66	59.40 ± 2.40	4.3 ± 0.7	180 ± 93

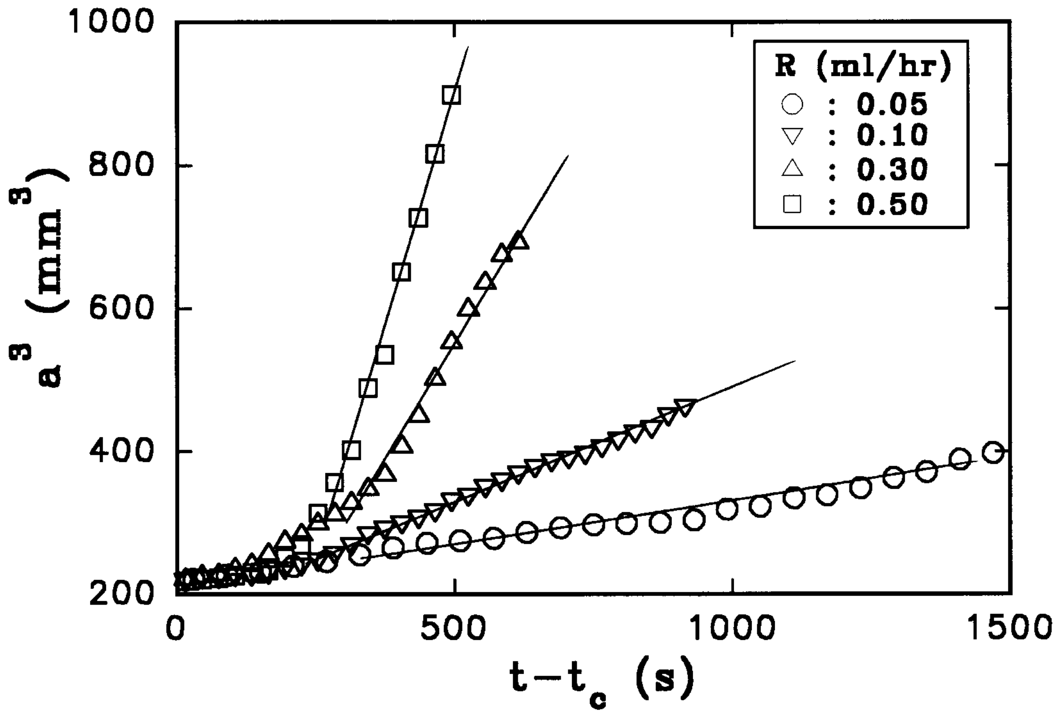

Figure 11 Variation of a^3 versus $t - t_c$ after debonding for the determination of M values, according to eq. 6.

taken into consideration. In other words, eqs. 1 and 2 may not be applicable to a higher flowrate.

After Debonding

After initiation of a debond, the apparent debonding rate, da/dt, and the height growth rate dy/dt were measured from Figures 3 and 4, respectively and were tabulated in Table III. As mentioned previously, initially a slow growth of the blister radius was observed until the pressure reached a maximum value where a fast crack growth proceeded. The debonding rate in the slow growth region is irrelevant to the flowrates, as shown in Table III. In the fast growth region, however, the debonding rate is increased from 1.32 to 12.2 μm/s when the flowrate is raised from 0.05 to 0.5 mL/h. The height growth rate dy/dt is also larger for a higher flowrate applied. However, they are all smaller than those before debonding takes place, as shown in Table I, at the corresponding flowrates.

The adhesive fracture energy G_a between the elastic tape and the PMMA plate can be determined from three methods, as mentioned in the theoretical section. According to the FK method, eq. 3, the only parameter needed to measure is the critical height y_c at which an initial circular debond starts to grow. However, the determination of y_c is never an easy task in considering the failure process. Fernando et al.[13] used the moment where a departure from linearity of p/y versus y^2 was observed to define the values of y_c and P_c. As shown in Figure 6, a relatively broad maximum of p/y variation is evident. The initiation of a debond can take place either before or at the maximum, depending on the relative increment of P and y as shown in Figures 4 and 5. A slightly smaller value of y_c is obtained when the suggestion by Fernando et al. is applied. Normally, the deflection of the blister height y is not large that a good estimated value of y_c still can be obtained. To obtain better results, the measured critical heights, y_c, in Table II were used. After substituting into eq. 3, the values of G_a were determined and tabulated in Table II as well. The deduced value of G_a is about 3.0 ± 0.5 J/m^2, regardless of the injected flowrates used.

For measurements of G_a using the GL method, values of Py product are plotted as a function of blister height after the debonding takes place, as shown in Figure 9. The arrows point to the moment where the maximum pressure occurs during the debonding process. As mentioned previously,

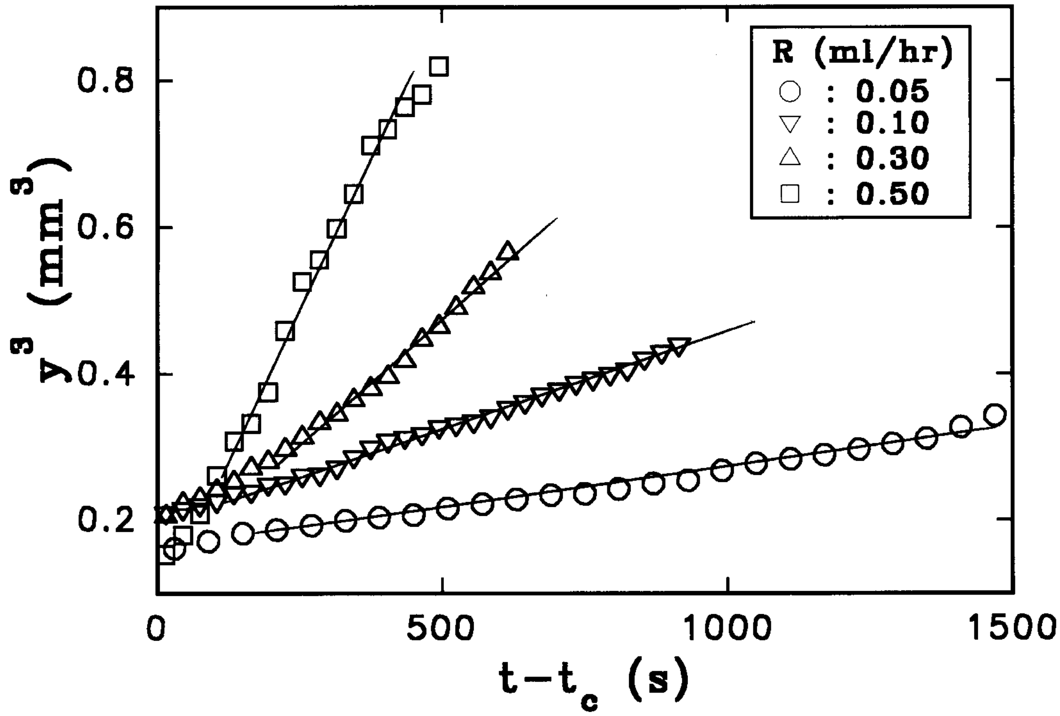

Figure 12 Variation of y^3 versus $t - t_c$ after debonding for the determination of L values, according to eq. 7.

a fast crack growth occurs after the pressure inside the blister reaches a maximum. As can be seen, a constant value of Py, as implied by eq. 4, is obtained exclusively in the fast crack growth region, especially for the case $R = 0.5$ mL/h. Moreover, the value of Py product is increased when a large flowrate is applied. Figure 10 shows the variation of Pa product with blister radius after the debonding occurs. Similarly, a large scatter in the measured values is found in the slow crack growth region. In the fast crack growth region, on the other hand, constant values of Pa product are obtained for each flowrate. Measured values of Py and Pa product are tabulated in Table IV. After substituting into eqs. 4 and 5, values of G_a and E are calculated and shown in Table IV as well. A slightly increase of G_a values, from 2.6 to 4.3 J/m^2, is found when the flowrate is increased from 0.05 to 0.5 mL/h. Therefore, effect of the debonding rate on the interfacial strength is not significant for a rate ranged from 1.3 to 12.2 μm/s. A relatively small elastic modulus of the tapes, 200 MPa, is found, compared with that obtained from FK method. However, one should be aware of the difference in theoretical basis between GL and FK methods. The former focuses on the crack growth region where debonding is taking place, i.e., a true fracture process. The latter uses the initiation of a debond to characterize the fracture behavior which will occur thereafter.

According to the CD method, a linear relation between a^3, y^3 and P^{-3} with $t - t_c$ is expected after the debonding takes place. Here, t_c is the critical time when a debond is initiated. Variations of a^3, y^3, $and\ P^{-3}$ with $t - t_c$ are shown in Figures 11, 12, and 13, respectively. It is apparent that linearity is observed only after the debond grows for a certain period until the maximum pressure is reached. The situation is more pronounced in Figure 13 where a minimum of P^{-3} is observed at the corresponding status. Thus, valid measurements should be made in the fast crack growth region. In other words, the time when the pressure reaches a maximum should be taken as t_c, instead of the time to initiate a debond. It should be noted, however, that the slope remains unchanged although a different definition of t_c is used. Chu et al.[15] used a "sequential debonding" technique to overcome the abnormal crack growth in their system, i.e., initially fast crack growth, followed by slow crack growth. In their analysis, the time to cause a second debond is used to define a reasonable t_c value. In fact, a larger

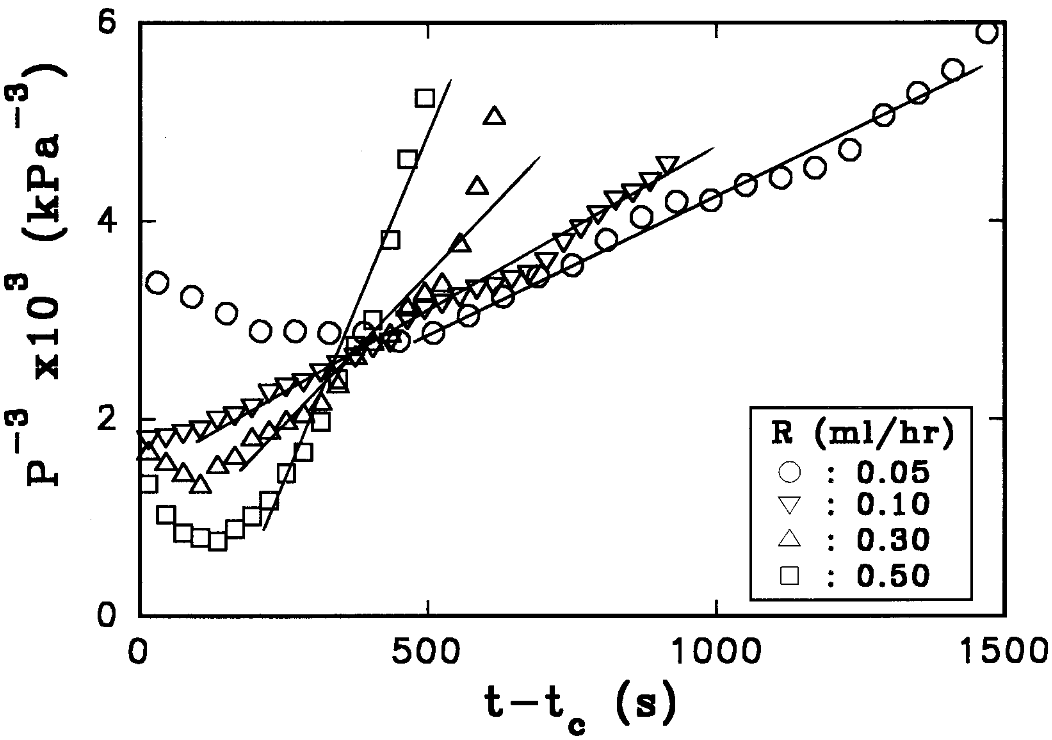

Figure 13 Variation of p^{-3} versus $t - t_c$ after debonding for the determination of N values, according to eq. 8.

blister radius a_o is applied when the sequential debonding technique is adopted. Similarly, the intercept of the a^3 axis may vary but the slope, da^3/dt, should remain unchanged, according to their theory.

Values of M, L, and N, determined from the linear slopes and tabulated in Table V, are increased when a large injected flowrate is applied. By substituting the values of M, L, and N into the corresponding equations (6, 7, and 8), the calculated values of G_a are shown in Table V as well. A large difference in the measured values, ranging from 0.2 to 16.7 J/m^2, is obtained when eqs. 6 and 7 are used. However, results derived from eq. 8 are consistent with those obtained from FK and GL methods. The large discrepancy is attributed to the insensitive dependence of blister radius and height on the fracture time. On the other hand, more accurate pressure data can be obtained using a sensitive pressure transducer which renders results more reliable.

To summarize, agreements in the measured values of G_a can be reached between FK and GL methods if the residual stress is small. Results calculated using the CD method show a large difference from those obtained from FK and GL methods, except when sensitive dependence of

Table V Measured Values Using the CD Method

R (mL/h)	M (mm^3 s^{-1})	$L \times 10^4$ (mm^3 s^{-1})	$N \times 10^6$ (kPa^{-3} s^{-1})	G_a (J/m^2) Eq. 6	G_a (J/m^2) Eq. 7	G_a (J/m^2) Eq. 8
0.05	0.126	1.501	2.960	1.2	16.7	1.6
0.1	0.286	2.545	3.079	0.7	12.0	2.1
0.3	1.021	6.720	5.060	0.3	9.3	2.7
0.5	2.240	14.80	13.77	0.2	16.3	2.2

E = 350 MPa.

pressure on the fracture time is measured and eq. 8 is applied.

As the flowrate of the injected fluid increases from 0.05 to 05 mL/h, the apparent rate of debonding is increased from 1.3 to 12.2 μm/s. An insignificant effect of debonding rate on the adhesive fracture energy was found in the present system.

CONCLUSION

To determine the interfacial strength between thin films and substrates, the blister test is an appropriate method due to the solid bases of the deformation theory. By measuring the dimensions of the blister (height and radius) and pressure inside the blister, the adhesive fracture energy, the residual stress and the elastic modulus of the thin film can be deduced in a single test. In this article, three different methods have been applied to analyze the adhesion of an elastic tape with a PMMA plate. An attempt is made to investigate the effect of the injected flowrate on the measured interfacial strength. Results show that consistent values of G_a and elastic modulus are obtained using FK and GL approaches. In contrast, a large deviation of measured G_a values has been found by CD method. Moreover, the flowrate of the injected fluid (thus, the debonding rate) does not show a pronounced effect on the data analysis for the present case. However, one has to consider the dynamic effect in order to derive reasonable results when the flowrate is too high that current equations based on the static deformation may become invalid. In general, the blister test is particularly important in the determination of the adhesion between photoresist and silicon substrate due to it delicate nature. Adhesion measurements of the photoresists used for 193 nm microlithography on different substrates are currently being conducted in this laboratory.

General financial support was provided by the National Science Council (R.O.C.) is greatly appreciated. Some of the measurements were carried out by J.-Y. Lin.

REFERENCES

1. Gent, A. N. J Adhesion 1987, 23, 115.
2. Andrews, E. H.; Kinloch, A. J. Proc R Soc London Ser A 1973, 332, 385.
3. He, M.-Y.; Hutchinson, J. W. Int J Solids Structures 1989, 25, 1053.
4. Gent, A. N.; Lai, S.-M. J Polym Sci Polym Phys 1994, 32, 1543.
5. Liu, G.; Gent, A. N. J Adhesion 1992, 38, 79.
6. Wang, S. S.; Yau, J. F. Int J Fracture 1982, 19, 295.
7. Reedy, E. D. Jr. Eng Fracture Mech 1991, 38, 273.
8. Gent, A. N.; Hamed, G. R. J Adhesion 1975, 7, 91.
9. Dannenberg, H. J Appl Polym Sci 1961, 5, 124.
10. Khan, M. B.; Briscoe, B. J. Polym Comp 1994, 15, 83.
11. Gent, A. N.; Lewandowski, L. H. J Appl Polym Sci 1987, 33, 1567.
12. Hinkley, J. A. J Adhesion 1983, 16, 115.
13. Fernando, M.; Kinloch, A. J. Int J Adhesion Adhesives 1990, 10, 69.
14. Coburn, J. C.; Pottiger, M. T.; Noe, S. C.; Senturia, S. D. J Polym Sci Polym Phys 1994, 32, 1543.
15. Chu, Y. Z.; Durning, C. J. J Appl Polym Sci 1992, 45, 1151.
16. Allen, M. G.; Senturia, S. D. J Adhesion 1988, 25, 303.
17. Julia-Schmutz, C.; Hintermann, H. E. Surf Coat Technol 1991, 48, 1.